12/20

FPRINT-93-04

FPRINT-93-04

Fermilab Library
0 1160 0021861 4

Signature of Supernova Neutrino Flavor-Mixing in Water Čerenkov Detectors

Yong-Zhong Qian and George M. Fuller

Department of Physics, 0319

University of California, San Diego

UC, San Diego

9500 Gilman Dr., La Jolla, CA 92093-0319

Abstract

We study supernova neutrino burst signals in large water Čerenkov detectors, examining the effects of any mixing between ν_e and either ν_μ or ν_τ, and taking account of charged-current ν_e capture on oxygen in the detector. We show that the characteristic count rates and angular distributions from supernova neutrino-induced events can depend sensitively on the degree of neutrino flavor-mixing. This sensitivity results from the different average energies expected in supernova models for ν_e on the one hand and ν_μ and ν_τ on the other, the steep increase in the O(ν_e,e)F cross section with neutrino energy, and the backward-peaked nature of the exit channel electron in this reaction. Neutrino flavor-mixing effects in supernova neutrino burst signals could be seen for a galactic supernova in the Super Kamiokande detector.

Signature of Supernova Neutrino Flavor-Mixing in Water Čerenkov Detectors

Yong-Zhong Qian and George M. Fuller

Department of Physics, 0319

University of California, San Diego

9500 Gilman Dr., La Jolla, CA 92093-0319

I. Introduction

In this paper we study what can be learned about neutrino flavor-mixing from the detection of a supernova neutrino burst event. Previous studies have concentrated on the effects of neutrino flavor-mixing on the Type II supernova explosion mechanism,[1,2] and analysis of the SN1987a neutrino signals.[3,4] The SN1987a case has been discussed extensively following the detection of its neutrinos by the Kamiokande II (KII) and IMB detectors.[5] Only 11 and 8 neutrino events were detected by the KII and IMB detectors respectively, and the data obtained cannot provide any reliable information about neutrino flavor-mixing without specific, and questionable, assumptions being made. Since the first event in the KII detector was forward-peaked, there were speculations that it was due to neutrinos from the earlier neutronization phase. Attempts to constrain neutrino flavor-mixing in supernovae were centered around this single event.[3,4] Haxton[6] has subsequently pointed out that the electron neutrino capture by oxygen in water Čerenkov detectors can have an important impact on the detection of high energy neutrinos. In turn, this reaction makes the neutrino detection event characteristics sensitive to any mixing between lower energy ν_e and higher energy ν_μ and ν_τ. We will show that neutrino

flavor-mixing has a readily detectable signature in the Super Kamiokande (SK) water Čerenkov detector for a galactic supernova.

We first discuss some aspects of neutrino emission from supernovae. Current supernova theory predicts that there will be two short pulses of neutrinos followed by a much longer pulse from a Type II supernova.[7] The short pulses consist of the neutrinos emitted during the infall and then those emitted when the shock reaches the neutrino-sphere. These are predominantly electron-neutrinos and they carry away an energy of a few 10^{51}ergs.[8] The "neutronization pulse" of neutrinos comes when the shock passes through the neutrino-sphere. The long pulse, or thermal emission phase, corresponds to the cooling and deleptonization of the hot proto-neutron star through thermal neutrino emission which consists of all six neutrino species. Almost all the gravitational binding energy of the new-born neutron star (of the order of 10^{53}ergs) is radiated away equally in these neutrino species. Each neutrino species has approximately a black-body type spectrum (Fermi-Dirac, zero chemical potential) characterized by the temperature of the "neutrino-sphere" for each species. The ν_μ and ν_τ's have a higher temperature than ν_e's, because the former decouple deeper in the core due to smaller opacities.[8] We take $T_{\nu_e} = T_{\bar{\nu}_e} =$ 5 MeV, and $T_{\nu_x} = T_{\bar{\nu}_x} = 7$ MeV ($x = \mu$ or τ) for the neutrino temperatures in the following discussion. Since the neutrino energy emitted in the neutronization phase is a few percent of that emitted in the thermal emission phase, the majority of the neutrino events in the detectors comes from the latter. Also, as far as neutrino flavor mixing is concerned, the presence of comparable numbers of all three neutrino

flavors in the latter makes the situation more interesting. Our main concern in this paper will be the neutrinos from the thermal emission phase.

II. Neutrino-Induced Events in Water Čerenkov Detectors

Now we turn to the neutrino events in existing water Čerenkov detectors such as the KII and IMB detetors from a supernova neutrino burst event. The main contribution to the neutrino events comes from $\overline{\nu}_e$ absorption on proton which is unaffected by neutrino flavor mixing, because there is no resonant level crossing in supernovae for the mixing between $\overline{\nu}_e$ and $\overline{\nu}_\mu$ or $\overline{\nu}_\tau$. The angular distribution of the positrons produced after the interaction is isotropic to a good approximation given the expected neutrino energies. With considerations of neutron recoil and forbidden effects of the same order, the actual distribution is slightly backward-peaked. Using the formulae given in reference [9], we find this angular distribution to be

$$P(\phi) = 0.5 - 0.051 \cos\phi \tag{1}$$

where ϕ is the angle between the incoming $\overline{\nu}_e$ and the outcoming positron. The second kind of neutrino events are due to ν–e scattering. The electrons are strongly forward-peaked after the scattering. From kinematics, the angle between the incoming neutrino and the recoil electron satisfies $\cos\phi > \sqrt{T/(T+2)}$, where T is the electron recoil kinetic energy in terms of the electron rest mass energy. For detection threshold energies exceeding 5 MeV in the KII and IMB detectors, $\cos\phi > 0.91$. The ν_e–e scattering cross-section is larger than ν_μ–e or ν_τ–e scattering cross-section since the ν_e–e channel has a charged-current contribution which the others lack.

Electron-neutrino absorption on natural oxygen can become important for water Čerenkov detectors, as pointed out by Haxton.[6] For ν_e temperature higher than 5 MeV, this process contributes more to the observed event rate than ν_e–e scattering. Haxton calculated O(ν_e,e)F weak strength function in detail and also computed the expected angular distribution of electrons from this process for the KII and IMB detectors. Like the angular distribution of positrons from $\overline{\nu}_e$ absorption on proton, the distribution of electrons for O(ν_e,e)F is also somewhat backward-peaked. However, the difference between the two is that the electron angular distribution for O(ν_e,e)F depends on the ν_e energy. The harder the ν_e energy spectrum is, the stronger the backward-peaked tendency will be. From Figure 2 given in reference [6], we find that for $T_{\nu_e} = 5$ MeV, the electron angular distribution is given by

$$P(\phi) = 0.492 - 0.394\cos\phi + 0.024\cos^2\phi \tag{2a}$$

for the KII detector and

$$P(\phi) = 0.493 - 0.407\cos\phi + 0.021\cos^2\phi \tag{2b}$$

for the IMB detector, whereas for $T_{\nu_e} = 7$ MeV, the electron angular distribution changes to

$$P(\phi) = 0.508 - 0.399\cos\phi - 0.024\cos^2\phi \tag{3a}$$

for the KII detector and

$$P(\phi) = 0.510 - 0.406\cos\phi - 0.030\cos^2\phi \tag{3b}$$

for the IMB detector. We calculate the effective cross-sections for ν–e scattering for the KII and IMB detectors and take other cross-sections from Table I given in reference [6], where ν_e–e scattering cross-sections are also given. These cross-sections are listed in Table I for two representative neutrino temperatures.

III. Neutrino Flavor Mixing in Supernovae

Neutrino flavor mixing is originally used to explain the so-called solar neutrino problem, and the most likely solution is the nonadiabatic one given by $\delta m^2 \sin^2 2\theta \approx 4 \times 10^{-8}$ eV^2 for $\delta m^2 = 10^{-7}$–10^{-5} eV^2, where δm^2 is the mass square difference and θ is the mixing angle.[10] Recent results from GALLEX experiment[11] narrow the range of δm^2 to 3×10^{-6}–10^{-5} eV^2. In connection with the dark matter problem, there are various particle physics models which try to justify the existence of a massive ν_τ with $m_{\nu_\tau} = 1$–100 eV. According to one specific model, i.e., the see-saw model,[12] such values of m_{ν_τ} would lead to a ν_μ mass right in the range to solve the solar neutrino problem. In this case, due to the large range of densities encountered in supernovae, ν_e's will go through two resonance regions in general, one for ν_e–ν_τ mixing in the mantle, the other for ν_e–ν_μ mixing in the envelope, as illustrated in Figure 1.

The nonadiabatic probability for an ν_e produced at high densities to remain as an ν_e after going through the resonance region is given by

$$P_{\nu_e \to \nu_e} = \exp\{-\pi H \delta m^2 \sin^2 2\theta / 4E\} \tag{4}$$

for $\theta \ll 1$, where E is the ν_e energy and $H = |d \ln \rho / dr|^{-1}_{res}$ is the density scale-height

at the resonance density ρ_{res} defined by

$$\frac{\delta m^2}{2E}\cos 2\theta = \sqrt{2}G_F N_A Y_e \rho_{res} \tag{5}$$

where symbles have their standard meanings. And the probability for an ν_e emitted at the neutrino-sphere to arrive at the detector as an ν_e is the product of the individual $P_{\nu_e \to \nu_e}$ for each resonance:[4]

$$P_{\nu_e \to \nu_e} = \exp\{-\pi(H_{12}\delta m_{12}^2 \sin^2 2\theta_{e\mu} + H_{13}\delta m_{13}^2 \sin^2 2\theta_{e\tau})/4E\} \tag{6}$$

The density scale-heights needed to calculate this probability are given in Table II for various neutrino energies for four representative δm^2's: 4×10^{-6} eV^2 and 8×10^{-6} eV^2 for ν_e–ν_μ mixing, and 225 eV^2 and 3600 eV^2 for ν_e–ν_τ mixing. For $\sin^2 2\theta_{e\mu}$, we incorporate the solution to the solar neutrino problem. As for $\sin^2 2\theta_{e\tau}$, different models[12,13] predict different values ranging from 10^{-7} to 10^{-3}. However, there are ways other than constructing particle physics models to investigate $\sin^2 2\theta_{e\tau}$. Fuller et al.[2] pointed out that if ν_τ has a mass range coincident with the required neutrino mass to close the universe, i.e., m_{ν_τ} = 10–100 eV, then there exists a resonance region for ν_e–ν_τ mixing above the neutrino-sphere where neutrinos are emitted and below the region where the unsuccessful shock is stalled. Fuller et al.[2] has shown that for $\sin^2 2\theta_{e\tau} > 4 \times 10^{-8}$, ν_e–ν_τ mixing results in at least an extra 60% increase in the shock energy in the late time neutrino reheating mechanism for supernova explosion. More recently, Qian and Fuller[14] show that if supernovae are the right site for the r-process nucleosynthesis of heavy

elements, then $\sin^2 2\theta_{e\tau} < 10^{-4}$–$10^{-6}$ for the corresponding $m_{\nu_\tau} = 1$–100 eV. Comparing these results with various predictions from particle physics models, we take $\sin^2 2\theta_{e\tau} = 10^{-6}$ in the following discussion. From observations of the SN1987a neutrino burst,[5] we can see that 70% of the neutrino signals in either the KII or the IMB detector were detected in the first 2 seconds. So we only take two instant density profiles of the mantle at tpb (time post bounce) = 0.177 and 0.638 sec to see the overall behavior of $P_{\nu_e \to \nu_e}$. The density profile of the envelope is almost static in the period of interest. However, any detailed calculation of neutrino flavor mixing effects has to take account of the time varying density structure of the supernova mantle. Any power law density profile is unrealistic for either the mantle or the envelope and can only be used as a crude approximation, because we need the density gradient in the calculation, not just the density.

IV. Calculation of Neutrino-Induced Events in Water Čerenkov Detectors

In the absence of neutrino flavor mixing, the expected number of neutrino events in the detector is given by

$$N(event) = N_{H_2O} \Phi_\nu \sigma_{eff} \tag{7}$$

where N_{H_2O} is the number of water molecules in the detector, Φ_ν the neutrino flux and σ_{eff} the effective cross-section.

$$\Phi_\nu = \frac{E_B/6}{< E_\nu >} \frac{1}{4\pi D^2} = 2.758 \times 10^{11} cm^{-2} (\frac{E_B}{10^{53} ergs})(\frac{MeV}{T_\nu})(\frac{10kpc}{D})^2 \tag{8}$$

where E_B is the gravitational binding energy of the new-born neutron star radiated in the thermal emission phase, $< E_\nu >$ the average neutrino energy, which is $3.152 T_\nu$

for a black-body type spectrum, and D the distance to the supernova.

$$\sigma_{eff} = n \int f_\nu \, dE_\nu \int \epsilon \, d\sigma \tag{9}$$

where n is the number of individual targets in one water molecule, f_ν the neutrino energy spectrum and ϵ the electron or positron detection efficiency of the detector.

$$f_\nu = \frac{1}{1.803} \frac{1}{T_\nu^3} \frac{E_\nu^2}{\exp(E_\nu/T_\nu) + 1} \tag{10}$$

and $\epsilon = 1 - \exp[-(E/E_{th})^p]$ where E is the electron or positron energy, E_{th}=9 MeV, p=3 for the KII detector and E_{th}=34 MeV, p=3.1 for the IMB detector.[6] Hence

$$N(event) = 9.219(\frac{E_B}{10^{53} ergs})(\frac{10kpc}{D})^2(\frac{M_{H_2O}}{kton})(\frac{Mev}{T_\nu})(\frac{\sigma_{eff}}{10^{-42} cm^2}) \tag{11}$$

where M_{H_2O} is the mass of water in the detector, which is 2.14 kton and 6.8 kton for the KII and IMB detectors respectively. Assuming $T_{\nu_e} = T_{\bar{\nu}_e} = 5$ MeV, $T_{\nu_x} = T_{\bar{\nu}_x} = 7$ MeV ($x = \mu, \tau$), $E_B = 2 \times 10^{53}$ ergs, D = 10 kpc, we give the expected number of events in Table III.

With neutrino flavor mixing, the number of scattering events and O(ν_e,e)F events will change. The increase in these events is given by

$$\delta N(\nu + e) = N_e \int (F^0_{\nu_x} - F^0_{\nu_e})(1 - P_{\nu_e \to \nu_e}) \, dE_\nu \int \epsilon \, [d\sigma(\nu_e + e) - d\sigma(\nu_x + e)] \tag{12}$$

where N_e is the number of electrons in the detector, and $F^0_\nu = \Phi_\nu f_\nu$. And

$$\delta N(\nu_e + O) = N_{H_2O} \int (F^0_{\nu_x} - F^0_{\nu_e})(1 - P_{\nu_e \to \nu_e}) \, dE_\nu \int \epsilon \, d\sigma(\nu_e + O) \tag{13}$$

Because the ν–e scattering cross-section increases approximately linearly with neutrino energy, and the neutrino fluxes reaching the detector scale roughly inversely with the individual average neutrino energies, even in the most favorable case of full conversion ($P_{\nu_e \to \nu_e} = 0$), the net increase in the total number of scattering events due to neutrino flavor mixing is small, being $\delta N(\nu + e) = 1$ and 2 for the KII and IMB detectors respectively. O(ν_e,e)F events are different in that the cross-section for this reaction increases rapidly with neutrino energy, which can easily overcompensate for the reduction in neutrino flux due to neutrino flavor mixing. This situation is illustrated in Figure 2 showing how the relative contribution of individual interaction to the neutrino events in the KII and IMB detectors as a function of neutrino temperature. From Figure 1 in reference [6], we find that the contribution to the O(ν_e,e)F events in the detectors mostly comes from ν_e's with energy around $E_{\nu_e} \approx 7.19 T_{\nu_e}$ for the energy spectrum we have assumed. To ensure a substantial conversion between ν_e's and ν_x's, we must have $P_{\nu_e \to \nu_e}$ as small as possible. As a rough criterion, we would like to have $P_{\nu_e \to \nu_e} \leq e^{-1}$ for $E_{\nu_e} = 50$ MeV. The scale-heights turn out to be $H_{12} \sim 10^{10}$ cm for ν_e–ν_μ resonance and $H_{13} \sim 10^6$ cm for ν_e–ν_τ resonance for the mixing parameters discussed above. And we can see that the criterion is satisfied. Therefore, we expect that full conversion between ν_e's and ν_x's is likely, and we give the expected number of events for this case in Table III also.

V. Discussion and Conclusion

As we can see from Table III, in both the KII and the IMB detector, the main

effect of neutrino flavor mixing is to increase the number of O(ν_e,e)F events. In fact, $\delta N(\nu+e) = 1$ and 2 whereas $\delta N(\nu_e+\mathrm{O}) = 25$ and 52 for the KII and IMB detectors respectively. It is interesting to notice that a substantial increase in O(ν_e,e)F events will signify the presence of neutrino flavor mixing as well as give us some hint to the ν_x energy spectrum such as what temperature the ν_x neutrino-sphere would have approximately.

Because we only have crude approximations for the neutrino energy spectra, the relative contribution from individual events is more reliable than the absolute numbers of individual events. We define the ratio of the number of O(ν_e,e)F events to that of p($\overline{\nu}_e, e^+$)n events to be f. We find that f increases from 1.66% and 1.55% without neutrino flavor mixing to 7.58% and 13.08% with full conversion of ν_x's into ν_e's for the KII and IMB detectors respectively. A difficult task now is to identify these additional neutrino events due to neutrino flavor mixing. As we explained previously, the ν–e scattering events are rather insensitive to neutrino flavor mixing. We shall neglect these events and concentrate on O(ν_e,e)F events in the following discussion.

First of all, the main product of O(ν_e,e)F is ^{16}F, which has no particle-bound states and decays to ^{15}O by proton emission almost spontaneously. ^{15}O then β^+ decays to stable ^{15}N with a half-life of 124 sec. The emitted proton is not detectable in the current water Čerenkov detectors and the emitted positron has a maximum energy well below the detection thresholds of both the KII and the IMB detector. Thus, these additional events cannot be identified by the afterward reactions.

The only hope seems to be the backward-peaked electron angular distribution for these events. Since ν–e scattering events are sharply forward-peaked, and we are interested in the backward-peaked events, neglect of the scattering events does not change our conclusion, and we shall study the angular distribution for the combined p($\overline{\nu}_e, e^+$)n and O(ν_e,e)F events only.

In the full conversion case, the angular distribution for these two events combined is given by

$$P(\phi) \approx 0.5 - 0.076 \cos\phi \tag{14a}$$

for the KII detector and

$$P(\phi) \approx 0.501 - 0.091 \cos\phi - 0.003 \cos^2\phi \tag{14b}$$

for the IMB detector. If there were no neutrino flavor mixing, the angular distribution in both detectors should be approximately given by equation (1). And we can distinguish these two cases as follows. Suppose we have N_0 events of p($\overline{\nu}_e, e^+$)n and O(ν_e,e)F in total. The difference in the number of events with $\cos\phi < 0$ between these two cases will be $\Delta N = 0.012N_0$ and $0.020N_0$ for the KII and IMB detectors respectively. Assuming no neutrino flavor mixing, there would be $N = 0.502N_0$ events with $\cos\phi < 0$. To distinguish these two cases, we must have $\Delta N > \sqrt{N}$, which means that we must have a total of 3486 and 1255 events of p($\overline{\nu}_e, e^+$)n and O(ν_e,e)F in the KII and IMB detectors respectively. Unfortunately, neither detector can satisfy this condition right now, the expected number of both events being 454 in the KII detector and 510 in the IMB detector for a galactic supernova 10

kpc away (see Table III). However, if we assume the SK detector is just an enlarged version of the KII detector, then the number of events will be 15 times larger ($M_{H_2O} = 32$ kton for the SK detector), and the above condition is easily satisfied. And this tendency of more backward-peaked events in the detector is the signature of neutrino flavor mixing we should look for.

Finally, we want to comment on the time delay effect on supernova neutrino signals in the water Čerenkov detectors due to a finite neutrino mass. Because neutrino flavor mixing is almost certain to occur if neutrinos have mass, we feel that a consistent discussion should include both effects of neutrino flavor mixing and time delay due to a finite neutrino mass. According to the see-saw model and the non-adiabatic solution to the solar neutrino problem, ν_e and ν_μ have negligible masses[10] and almost suffer no time delay effects for a distance of 10 kpc. Only ν_τ is massive enough to cause such an effect. Thus, the possible time delay effect can only be observed in the forward-peaked scattering events, and this effect does not affect our above discussion of the signature of neutrino flavor mixing. Of course, we have only discussed neutrino events from the thermal emission phase. As for the ν_e's from the neutronization phase, they will be converted into ν_τ's when arriving at the detector. Not only will these neutrinos be less likely to be detected due to the characteristically small scattering cross-section with electrons, but they will also suffer a time delay due to their much heavier mass and the induced scattering events will be accordingly dispersed, which makes the neutrino events from the neutronization phase even more difficult to identify.[15]

In conclusion, we find that the number of O(ν_e,e)F events in water Čerenkov detectors is very sensitive to neutrino flavor mixing in supernovae. And given that the SK detector is in full operation when the next galactic supernova explodes, the unique neutrino energy dependent backward-peaked angular distribution of these events will lead to an observable signature of supernova neutrino flavor mixing in the SK detector.

Acknowledgements

We want to thank J. R. Wilson for providing us with the density profiles from his supernova code. Y.-Z. Qian thanks the Institute for Nuclear Theory at University of Washington, Seattle for the opportunity to present an earlier version of this work at the supernova workshop in Feburary 1992. He also acknowledges discussions with W. C. Haxton and J. Pantaleone. This work was supported by NSF grant PHY-9121623 and Calspace grant CS-56-91.

References

[1]G. M. Fuller, R. W. Mayle, J. R. Wilson and D. N. Schramm, Astrophys. J. **322**, 795 (1987).

[2]G. M. Fuller, R. W. Mayle, B. S. Meyer and J. R. Wilson, Astrophys. J. **389**, 517 (1992).

[3]J. Arafune, M. Fukugita, T. Yanagida and M. Yoshimura, Phys. Rev. Lett. **59**, 1864 (1987); S. P. Rosen, Phys. Rev. D **37**, 1682 (1988). A brief review on this subject can be found in T. K. Kuo and J. Pantaleone, Rev. Mod. Phys. **61**, 937 (1989).

[4]T. K. Kuo and J. Pantaleone, Phys. Rev. D **37**, 298 (1988).

[5]K. S. Hirata et al, Phys. Rev. Lett. **58**, 1490 (1987); R. M. Bionta et al, Phys. Rev. Lett. **58**, 1494 (1987).

[6]W. C. Haxton, Phys. Rev. D **36**, 2283 (1987).

[7]H. A. Bethe, in *Highlights of Modern Astrophsics*, edited by S. L. Shapiro and S. A. Teukolsky (John Wiley & Sons, New York, 1986).

[8]A. S. Burrows, in *Supernovae*, edited by A. G. Petschek (Springer-Verlag, New York, 1990).

[9]J. N. Bahcall, *Neutrino Astrophysics* (Cambridge University Press, New York, 1989).

[10]H. A. Bethe and J. N. Bahcall, Phys. Rev. D **44**, 2962 (1991).

[11]GALLEX Collaboration, Phys. Lett. B **285**, 390 (1992).

[12]S. A. Bludman, D. C. Kennedy, and P. G. Langacker, Center for Particle Astrophysics, Berkeley Report No. CfPA-Th-91-003 Rev (unpublished).

[13]S. Dimopoulos, L. J. Hall, and S. Raby, Lawrence Berkeley Laboratory Preprint LBL-32484.

[14]Y.-Z. Qian and G. M. Fuller, Bull. Amer. Astron. Soc. (to be published).

[15]H. Minakata and H. Nunokawa, Phys. Rev. D **41**, 2976 (1990).

TABLE I. Effective cross-section σ_{eff} for ν events. These cross-sections are in units of 10^{-42} cm^2. Numbers in the upper two rows are for the KII detector,and those in the lower ones are for the IMB detector.

$T(MeV)$	p$(\overline{\nu}_e, e^+)$n	O$(\overline{\nu}_e, e^+)$N	$e\overline{\nu}_e \rightarrow e'\overline{\nu}'_e$	$e\overline{\nu}_x \rightarrow e'\overline{\nu}'_x$	$e\nu_x \rightarrow e'\nu'_x$	$e\nu_e \rightarrow e'\nu'_e$	O$(\nu_e$,e)F
5	52.9	0.609	0.195	—	0.120	0.785	0.829
7	—	—	—	0.167	0.208	1.34	5.63
5	17.8	0.213	0.0181	—	0.0153	0.105	0.297
7	—	—	—	0.0339	0.0442	0.303	3.31

TABLE II. Density scale-heights $|d\ln\rho/dr|^{-1}$ at resonance. $|d\ln\rho/dr|^{-1}$ values in the first two columns are for resonance in the envelope,those in the two middle columns are for resonance in the mantle at tpb = 0.177 sec and those in the last two columns are for resonance in the mantle at tpb = 0.638 sec.

δm^2(eV^2)	4×10^{-6}	8×10^{-6}	225	3600	225	3600
E(MeV)	$\times10^{10}(cm)$	$\times10^{10}(cm)$	$\times10^{6}(cm)$	$\times10^{6}(cm)$	$\times10^{5}(cm)$	$\times10^{5}(cm)$
2	1.074	0.852	4.083	1.013	2.04	0.4906
2.828	1.094	1.070	3.06	1.11	2.61	0.815
3.999	0.992	1.074	6.84	0.787	2.71	0.576
5.654	1.008	1.094	6.94	1.509	4.19	1.324
7.995	1.062	0.992	7.1	1.89	4.88	0.936
11.31	1.061	1.008	10.8	2.412	3.45	2.52
15.99	0.815	1.062	15.7	2.91	4.53	3.20
22.60	0.497	1.061	14.9	3.07	6.53	2.89
31.96	1.023	0.815	19.87	4.33	4.62	2.041
45.19	1.958	0.497	11.7	4.37	7.354	2.62
63.90	2.167	1.023	8.27	4.66	9.83	2.72
90.36	2.541	1.958	7.6	6.95	6.96	4.194
127.8	3.516	2.167	5.38	7.11	14.4	4.88
180.7	4.269	2.541	3.8	10.85	10.21	3.453
255.5	4.217	3.516	12.8	11.07	37.0	4.537
361.2	5.565	4.269	9.03	14.9	28.6	6.53

TABLE III. Expected number of neutrino events in the KII and IMB detectors. $P_{\nu_e\rightarrow\nu_e} = 1$ refers to the case without neutrino oscillation and $P_{\nu_e\rightarrow\nu_e} = 0$ means full conversion of ν_e and $\nu_{\mu,\tau}$ into each other. Numbers in the upper two rows are for the KII detector,and those in the lower ones are for the IMB detector.

$P_{\nu_e\rightarrow\nu_e}$	$\overline{\nu}_e$absorption events	$e\nu \rightarrow e'\nu'$	O$(\nu_e$,e)F	Total
1	422	12	7	441
0	422	13	32	467
1	451	6	7	464
0	451	8	59	518

Figure Caption

Figure 1. Illustration of neutrino flavor mixing in supernovae.

Figure 2. Relative contribution of individual interaction to the neutrino events in the water Cĕrenkov detectors as a function of neutrino temperature. Solid line is for O(ν_e,e)F, dotted line for O($\overline{\nu}_e, e^+$)F, dash line for ν_e–e scattering, long dash line for p($\overline{\nu}_e, e^+$)n, and dot-short dash line for ν_x–e ($x = \mu$ or τ) scattering. Figure 1a is for events in the KII detector, and Figure 1b is for events in the IMB detector.

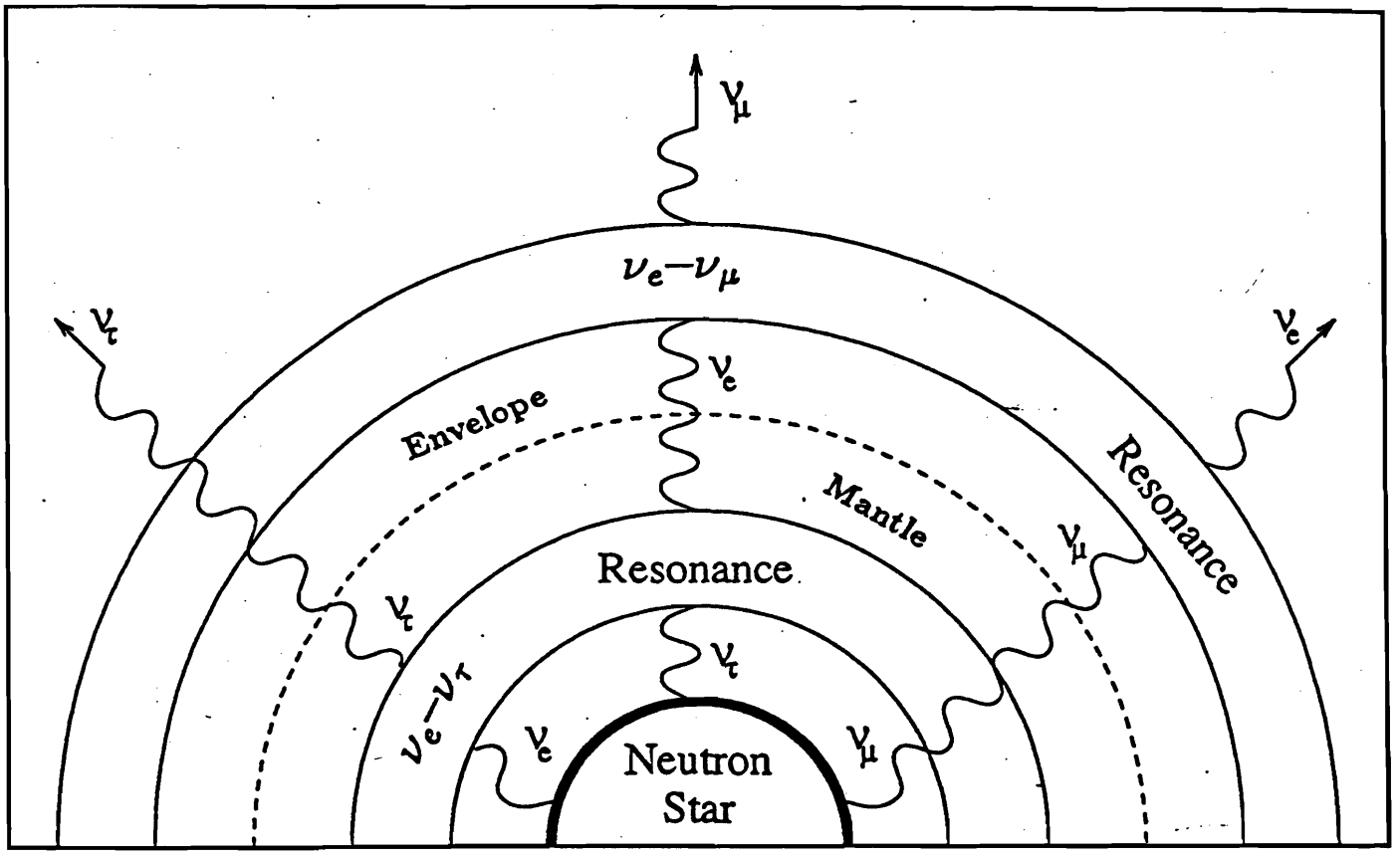
ν_μ
$\nu_e - \nu_\mu$
ν_τ
ν_e
ν_e
Envelope
Mantle
Resonance
ν_μ
Resonance
ν_τ
ν_τ
$\nu_e - \nu_\tau$
ν_e
ν_μ
Neutron
Star

Figure 1

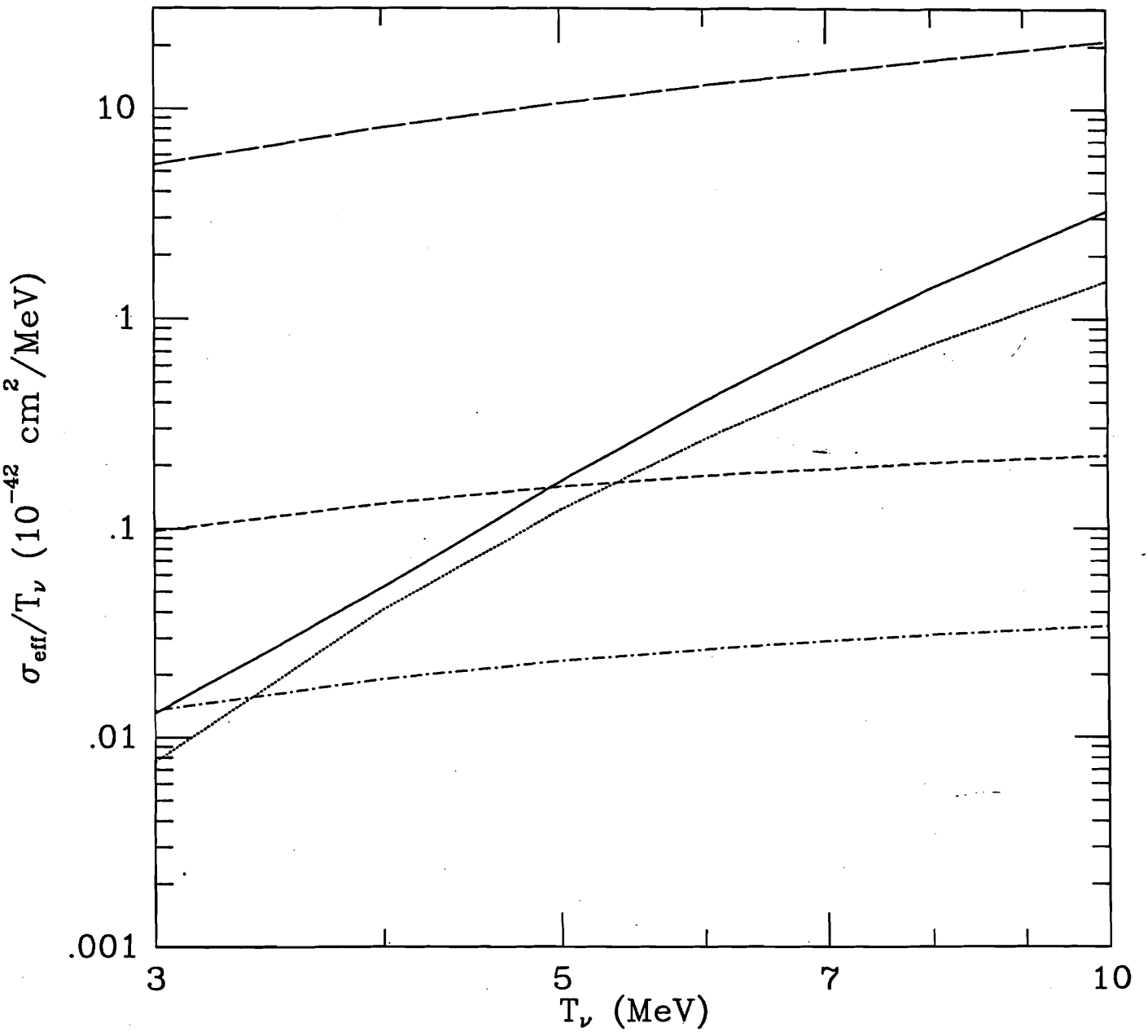

Figure 2a

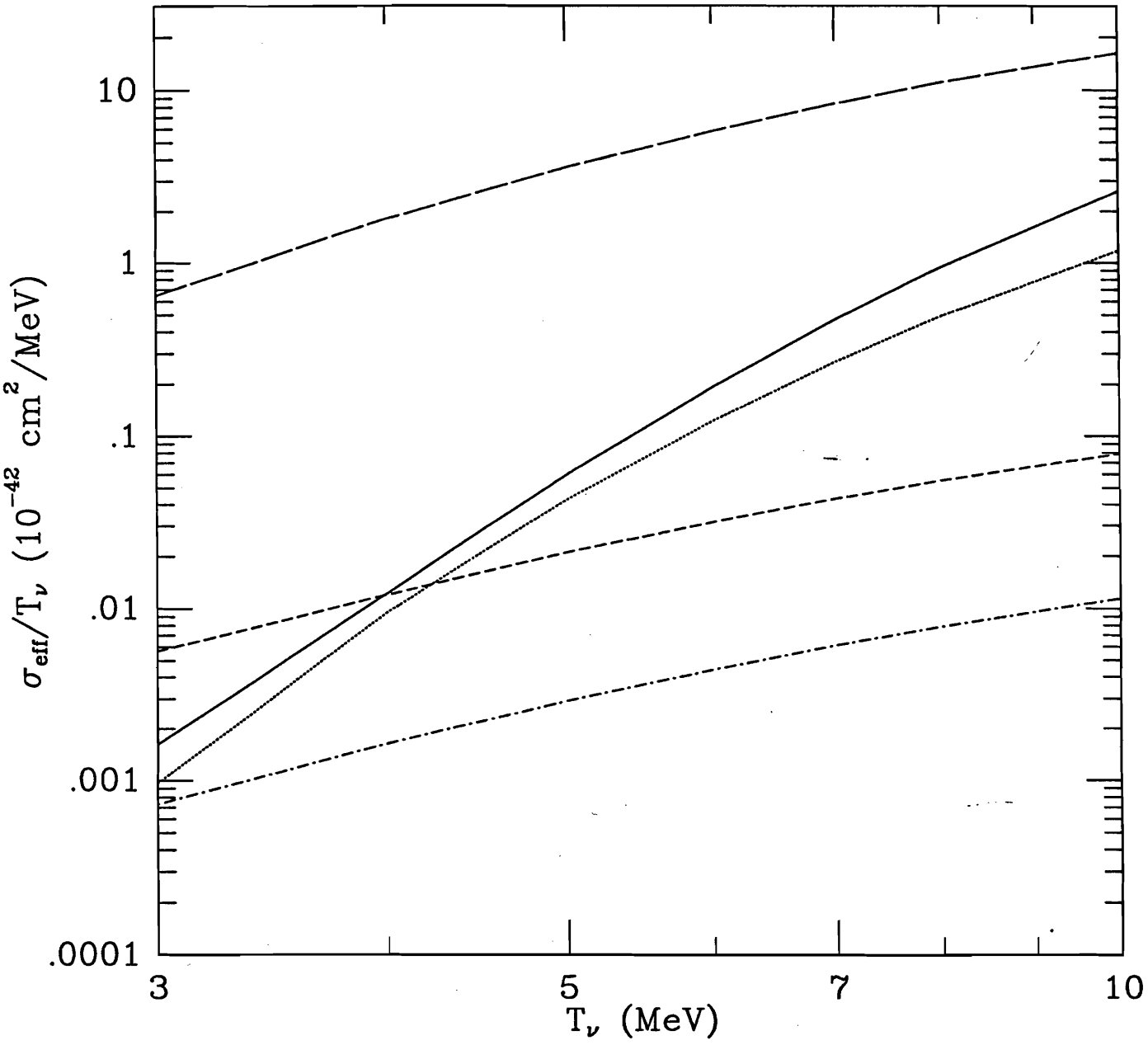

Figure 2b